A Novel Back-Support Exoskeleton With a Differential Series Elastic Actuator for Lifting Assistance

Shuo Ding, Francisco Anaya Reyes, Shounak Bhattacharya, Ashwin Narayan, Shuaishuai Han, Ofori Seyram, and Haoyong Yu, *Senior Member, IEEE*

***Abstract*—Compared to conventional back-support exoskeletons (BSEs) with two motors, BSEs driven by a single motor have the advantage of light weight. However, current single-motor BSEs have problems with accommodating asynchronous hip movements, achieving precise force control and efficient force transmission, and giving autonomy to users when walking. In this article, we propose a novel BSE with a differential series elastic actuator (D-SEA) for lifting assistance. The unique differential working principle can accommodate the angular difference between the hip joints and provide the same assistive torque at both hip joints. The D-SEA achieves precise force control with a custom controller based on accurate spring deflection feedback, and drives the hip joints via an efficient cable-roller mechanism. Taking advantage of the active backdrivability of the D-SEA, we proposed an intelligent assistive strategy that automatically provides adequate support for lifting tasks and grants autonomy to users during walking. In experiments, the BSE reduced the activation level of the back muscles by up to 40% during lifting, without increasing the activation of the back and leg muscles during walking.**

***Index Terms*—Back-support exoskeleton (BSE), differential series elastic actuator (D-SEA), lifting works, low back injuries.**

I. Introduction

LOW back injuries are the most common work-related musculoskeletal disorder (MSD) and require at least one week to recover [1]. Due to direct medical expenses and indirect costs of absenteeism, low back injuries cause more than $200 billion economic losses per year [2]. In many workplaces, such as warehouses, construction sites, airports, and hospitals, workers have to maintain prolonged awkward postures while bending to lift heavy objects, leading to a high risk of low back injuries [3]. The gravity of objects causes high load on the lumbar spine of workers (at L5/S1 area of the spine), which causes the back muscle to become fatigued and even damaged [4]. With the social trend of aging society and low fertility, protecting workers from low back injury has become an urgent issue for the industry. In recent years, devices that can reduce the load of the lumbar spine have been extensively studied. One example is back-support exoskeletons (BSEs) that are worn by the user and can provide assistive torque between the trunk and thigh (at the hip joints) [5]. As an on-body-device with a high level of flexibility, BSEs are more acceptable to workers than traditional off-body devices (such as hoists) [6].

Due to the advantage of lightweight and low cost, passive BSEs that use springs, carbon fiber beams, and elastic bands to generate the assistive torque are first applied [7]. However, a serious limitation of passive BSEs is that their assistive torque is determined by the intrinsic property of the elastic elements and cannot be modulated. Therefore, active BSEs with sensing and control systems are developed to modulate the assistance [8]. Active BSEs commonly use two motors to drive the left and right hip joints to provide assistance, such as the active pelvis orthosis (APO) [9], the XoTrunk [8], [10], the commercial BSE Cray X [11], and the asymmetric back exosuit (ABX) [12]. Unfortunately, the two-side motors and the transmission mechanisms often lead to a heavy prototype, which has become a major challenge of the active BSE. In addition, the use of two independent motors makes it difficult to provide the same assistive torque on both sides in lifting works (especially when the legs are staggered), which may cause discomfort due to the unbalanced assistance [13]. Therefore, the use of a single motor to reduce the weight of the device and provide the same assistance on both sides has become a new development trend in BSE.

To use one motor to assist the lifting work, the BSE design must meet the following requirements. First, the BSE should allow for the angular difference between the left and right hip joints (asynchronous hip movements) while providing the same

Manuscript received 16 July 2023; accepted 17 October 2023. Date of publication 9 November 2023; date of current version 16 January 2024. This paper was recommended for publication by Associate Editor Samer Mohammed and Editor Eiichi Yoshida upon evaluation of the reviewers' comments. This work was supported by the Science and Engineering Research Council, Agency of Science, Technology and Research, Singapore, through the National Robotics Program under Grant M22NBK0108. *(Corresponding author: Haoyong Yu.)*

This work involved human subjects or animals in its research. Approval of all ethical and experimental procedures and protocols was granted by Institutional Review Board of the National University of Singapore under Application No. LH-20-021, and performed in line with the Research Compliance Policy on Human Subject and Biomedical Research.

Shuo Ding, Francisco Anaya Reyes, Shounak Bhattacharya, Ashwin Narayan, and Ofori Seyram are with the Department of Biomedical Engineering, National University of Singapore, Singapore 117583 (e-mail: dingshuo@zju.edu.cn; bme.fco.anaya@gmail.com; bhsapiens91@gmail.com; ashwin_narayan@u.nus.edu; e0787983@u.nus.edu).

Shuaishuai Han and Haoyong Yu are with the Department of Biomedical Engineering, National University of Singapore, Singapore 117583, and also with the National University of Singapore (Suzhou) Research Institute, Suzhou 215123, China (e-mail: ss.han@njust.edu.cn; bieyhy@nus.edu.sg).

This article has supplementary material provided by the authors and color versions of one or more figures available at https://doi.org/10.1109/TRO.2023.3331680.

Digital Object Identifier 10.1109/TRO.2023.3331680

IEEE Transactions on Robotics (T-RO) paper, presented at ICRA 2024, Yokohama, Japan. Cite as T-RO paper.

assistive torque. Second, good quality force control (to provide the desired force to the user) and efficient force transmission (to save motor power) must be achieved even with a single motor [14], [15]. Third, the BSE should automatically distinguish lifting works from walking so that the user can walk without the resistance from the device [7]. However, current BSEs with a single motor still struggle to meet the abovementioned requirements. The BSE of [16] used one motor (with a ball screw, placed on the human back) and Bowden cables to generate the same torque at two hip joints, but it cannot allow their angular difference. When wearing the device, the user can only perform synchronized hip movements, which causes great inconvenience. The BSE H-WEX [17] used a gear mechanism and cables to transfer the force to two hip joints (from one motor), but an inherent limitation of the device is the cable slack problem due to the unidirectional force transmission of the cable (in the direction of hip extension). Therefore, an improved version of H-WEX (called H-WEX-v2) is developed with bidirectional force transmission achieved by a complex cable-roller mechanism [13]. However, the force control accuracy of H-WEX-v2 is affected by the indirect estimation of the spring deflection (the force is controlled by the spring based on Hooke's law), due to the accumulation of sensor's errors and the elasticity of the cable. In addition, the force transmission mechanism of the H-WEX-v2 has a low efficiency, with an unavoidable loss of 13% of the cable force. More importantly, the H-WEX-v2 only allows free hip movements with the same amount in the opposite direction, which generates walking resistance, since human gait is asymmetric and the average of the left and right hip flexion angles varies between 10° and 20° during walking [18].

To overcome the abovementioned challenges, in this work, we proposed a novel lightweight BSE with a differential series elastic actuator (D-SEA) for lifting work assistance. The unique differential working principle of the D-SEA can provide the same amount of assistive torque at both hip joints regardless of the angular difference. Based on feedback from a high-precision linear encoder that directly measures spring deflection, the D-SEA achieves precise force control with a custom controller. In addition, an efficient cable-roller mechanism is designed to transmit force to the hip joints with small force loss (only the friction of rollers). The proposed BSE has two unique features to allow the user to walk without the resistance of the device. First, the D-SEA can achieve active backdrivability (accurate zero force tracking) to allow the user to master the motion in free mode (human-in-charge mode). Second, an intelligent assistive strategy was proposed to smoothly switch between free mode (for walking) and assist mode (for lifting works) based on the user's movement information. When assisting lifting works (assist mode), the BSE can provide appropriate assistance according to user's needs with a virtual impedance controller. A series of experiments have been performed to validate the proposed approach.

Due to the D-SEA, our BSE can achieve the following advantages compared with existing BSEs, which are the main contributions of this work.

1) The proposed BSE has good portability and is one of the lightest active BSEs, as shown in Table I.
2) The BSE can provide desired assistance to users thanks to good quality force control and real-time feedback on movement information. Moreover, through the D-SEA, users can obtain the same (balanced) assistive torque at the hip joints during lifting, improving user comfort.
3) Users can walk freely after lifting up the object, which is of great significance for workplaces where workers need to transport objects.

TABLE I
CURRENT ACTIVE BSES

Name	Weight	Torque (rated)	Torque (max)
APO [9]	8 kg	20 Nm	NA
XoTrunk [8], [10]	6 kg	40 Nm	NA
Cray X [11]	7 kg	NA	NA
ABX [12]	6.4 kg	20 Nm	100 Nm
BSE in [16] external power	4.4 kg	20 Nm	27.3 Nm
H-WEX-v2 [13]	5.5 kg	30 Nm	94.5 Nm
Our BSE	5.3 kg	30 Nm	70 Nm

[1] The torque refers to the total assistive torque of the device (the motor torques are summed for prototypes with two motors).

The rest of this article is organized as follows. Section II presents the working principle and design of the BSE. Section III presents the D-SEA control and the assistive strategy. Section IV describes several experiments performed to validate the proposed device. The results of the experiments are discussed in Section V. Finally, Section VI concludes this article.

II. EXOSKELETON DESIGN

A. Working Principle of the BSE

Fig. 1(a) shows a user wearing the proposed BSE to lift loads. When the user lifts the object, the gravity of the upper body and the object causes a large load on the lumbar spine (L5/S1 area). To overcome the load, the worker must generate a large flexion torque through the spinal erector. Since the moment arm of the spinal erectors force is much smaller than that of the gravity load, the spinal erectors have to provide a huge compressive force and are prone to injury due to overstress and overfatigue. In addition, the large stress on the lumbar spine also increases the risk of spinal injury [19]. The BSE aims to reduce the load on the lumbar spine, which can effectively protect the user from back injuries.

The working principle of the BSE (the model is built in the sagittal plane) is shown in Fig. 1(b). The BSE consists of a main frame, a D-SEA, two hip joints (left and right), two thigh links, cables and rollers. The main frame and thigh links are attached to the human back and legs by means of straps and are rotatably coupled to the hip joints. The cables are connected between the D-SEA and the hip joints through the rollers (each hip joint is connected with two cables). During lifting, the D-SEA pulls the cable in the hip extension direction and generates an assistive torque at both hip joints. The sum of the left and right assistive torque (τ) helps to reduce the load on the lumbar spine. In the shoulder position, the main frame provides a supporting force on the user's upper body (F_H). A compressive force (F_T) is

IEEE Transactions on Robotics (T-RO) paper, presented at ICRA 2024, Yokohama, Japan. Cite as T-RO paper.

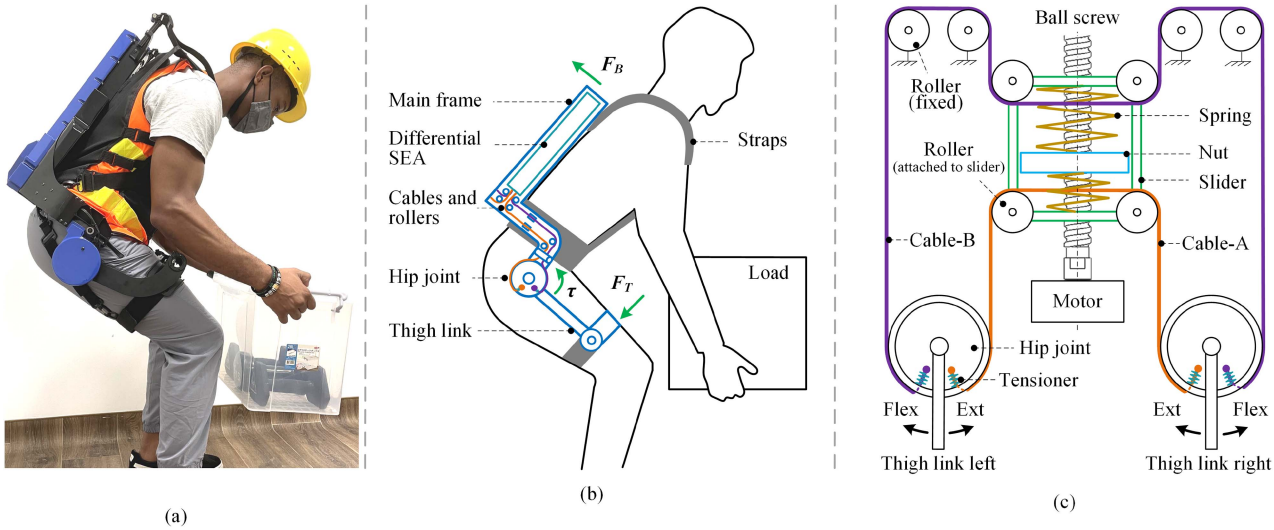

Fig. 1. (a) User wears the proposed BSE to lift loads. (b) Working principle of the proposed BSE (the model is built in the sagittal plane). (c) Working principle of the D-SEA. The motor drives the ball screw nut to compress the spring and pushes the slider to move upward. Cable-A is then pulled, producing the same driving force (extension torque) on both hip joints. The displacement of the slider depends on the average value of the hip flexion angles. The difference between the two hip flexion angles is automatically compensated by the sliding of the cables along the rollers.

also applied to the thighs via the thigh links and cuffs. The BSE redistributes part of the load from the lumbar spine to the user's shoulders, chest, and thighs. By using soft straps with a large contact area, we can reduce the stress on the user's body to avoid discomfort.

B. Working Principle of the D-SEA

The operating principle of the D-SEA is shown in Fig. 1(c). The D-SEA mainly consists of a motorized ball screw, a slider, springs, cables, rollers, and tensioners. The slider is mounted on a linear guide and can move along the ball screw. The springs are mounted between the slider and the ball screw nut. We choose two different springs here, one large and one small (with the same stiffness but different lengths), to save space since we only apply a large force in the direction of extension of the hip joint. In addition to the rollers attached to the slider, other rollers are attached to the main frame to guide the cables. Although we used two cables (cable-A and cable-B) to provide a two-way drive, the problem of cable slack can still occur due to the elasticity of the cable. As soon as a large force is applied to one cable, making it slightly longer, the other cable becomes slack. Therefore, small compression springs are attached to the end of the cables to act as tensioners to prevent the cables from sagging. The cable-roller mechanism has high force transition efficiency since all cables move along the rollers with low friction.

Differential actuation is achieved as follows. The motor drives the ball screw nut to compress the spring [for example, the large spring in Fig. 1(c)] and pushes the slider to move upward. Cable-A is then pulled, producing driving force on both hip joints. Since the force on the same cable is equal, the torque at both hip joints are always the same. The displacement of the slider depends on the average value of the hip flexion angles. The difference between the hip flexion angles is automatically compensated by the sliding of the cables along the rollers. The cable force is half of the spring force, which can be controlled based on the spring deflection feedback via Hook's law. By directly measuring the spring deflection with a high-precision sensor, we developed a suitable controller to achieve the accurate force control of the D-SEA.

C. Prototype Design

The overall structure of the BSE is shown in Fig. 2(a). The D-SEA is installed on the main frame (covered by a back shell), which is attached to human back with straps. At the top of the main frame are two sliding links (usually fixed with screws) that can be used to adjust the height of the device. One end of the thigh link is attached to the hip joint (diameter: 100 mm), and the other end is connected to the human leg via the thigh cuff and straps. A battery box and a controller box are also attached to the main frame to hold the electronic components.

The structural details of the D-SEA are shown in Fig. 2(b). A servo motor (RMD-L-5015, TAMAI Company, Ltd., power 120 W) is used as the prime mover (with integrated encoder and driver) to drive the ball screw (C-BSSH1205, MiSUMi, pitch: 5 mm) through a coupling. A RLM2 noncontact magnetic linear encoder (from RLS, Slovenia) with high resolution is used to measure the spring deflection. Real-time control is implemented on a custom-built embedded control board with small size [see Fig. 2(c), 65 × 30 × 30 mm]. A switch allows the user to manually turn-OFF the device. All electrical components are powered by a lithium polymer battery placed in the battery box (with 6 cells in series, capacity: 3300 mAh, weight: 0.5 kg, operation time: around 4 h in experiments). Cable-A and cable-B are connected between the slider and the hip joints. The cable path is passed through the roller mechanism, as shown in Fig. 2(d) (some components are hided to clearly show the cable path).

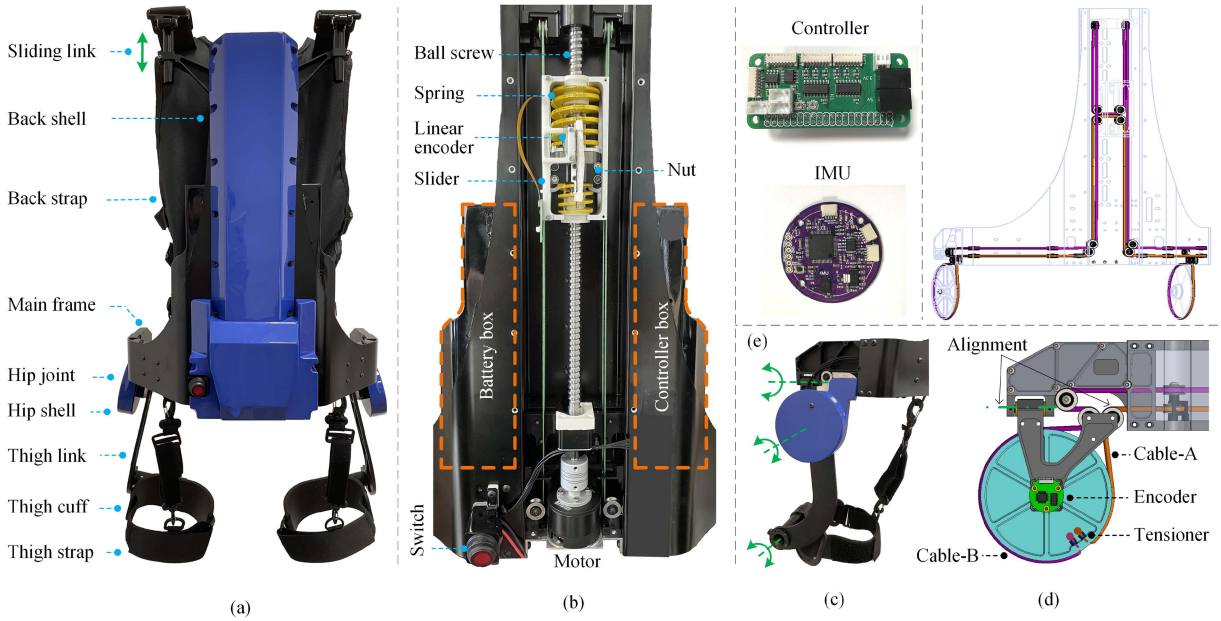

Fig. 2. (a) Overall structure of the BSE. (b) Structural details of the D-SEA (inside the back shell). (c) Main components inside the controller box. (d) Cable path inside the main frame (some components are hided to clearly show the path). (e) DOFs and structural details of the hip joint (with the hip shell hided).

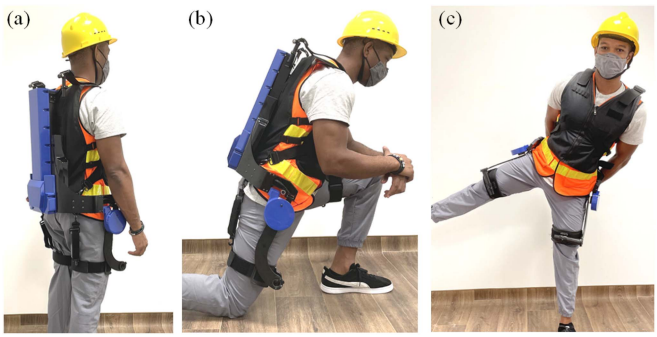

Fig. 3. User wears the BSE. (a) Standing straight. (b) Striding. (c) Kicking the leg to one side.

There are a total of three degrees of freedom (DOFs) on each side of the BSE as shown in Fig. 2(e), including hip flexion/extension, hip abduction/adduction, and a rotational DOF between the thigh link and the cuff. We placed the centerline of hip abduction/adduction tangential to the edge of the roller where the cable passes, therefore, hip abduction/adduction does not affect the force transfer of the cable. The DOF between the thigh link and the cuff allows the thigh cuff to rotate with the thigh for comfort. The hip flexion/extension angle is measured with an RMB20 noncontact magnetic encoder from RLS (Slovenia). In addition, a customized inertial measurement unit [IMU, see Fig. 2(c)] is integrated into the controller box to measure upper body postures. Fig. 3 shows a user wearing the BSE with some typical movements.

We placed the relatively heavy components, such as the battery and motor, at the bottom of the D-SEA to lower the center of gravity of the device so that the torque caused by the weight of the device acts in the same direction as the assistive torque when the user bends down. We chose carbon fiber and aluminum alloy 7075 as the material for the structural parts and the shells are 3-D printed with ABS plastic. To accommodate different body shapes, the prototype is made in different sizes, such as S, M, and L. In the experiments, the nominal assistive torque is 30 N · m (determined by the current springs with a stiffness of 55 N/mm) and is close to that of the APO (20 N · m, [10]) and the H-WEX-v2 (30 N · m, [13]). If harder springs are used, the maximum assistive torque of the BSE can reach up to 70 N · m.

III. Exoskeleton Control

A. Control of the D-SEA

Force control should be applied to the exoskeleton rather than position control to provide the desired force directly to the user [14]. Based on the linear force dynamics of the D-SEA, we have developed a disturbance-resistant force controller for human assistive applications. Such a controller consists of a feedforward control term, a PD-type feedback control term, and a disturbance observer (DOB). By providing real-time estimation of the disturbance, the DOB helps mitigate the negative effects, such as friction, backlash, and forces from human (plant model variations and external disturbances), and tries to maintain the characteristic response of the nominal model. In addition, the DOB can reduce the steady-state error, which serves as an integral feedback term to simplify the feedback term design of the controller. The DOB has been shown to improve the torque tracking capability of SEAs [20].

The model of the D-SEA is shown in Fig. 4(a). The dynamics of the motor and the ball screw can be built as

$$(J_m + J_b)\ddot{\theta}_m = \tau_m - b_m\dot{\theta}_m - \tau_b \quad (1)$$

where J_m and J_b are the moment of inertia of the motor and ball screw; θ_m is the motor rotation angle; τ_m is the motor torque

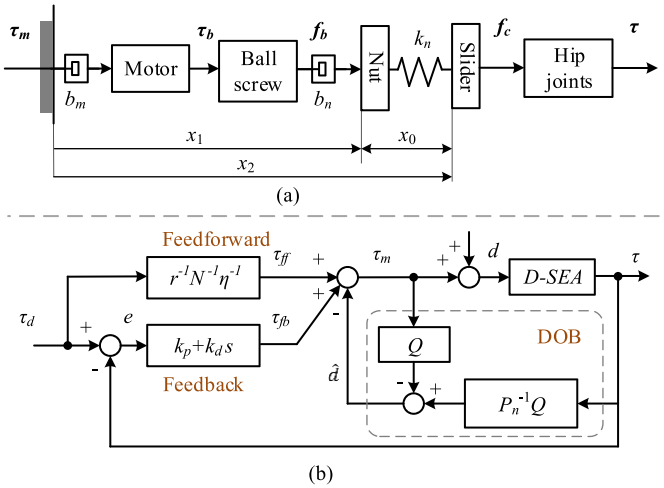

Fig. 4. (a) D-SEA model. (b) D-SEA controller.

command; b_m is the equivalent motor-side damping; τ_b is the torque on ball crew.

Considering the transmission efficiency of the ball screw (η), the output force of the ball screw (f_b), and the displacement of the ball screw nut (x_1) can be given by

$$f_b = N\eta\tau_b$$
$$x_1 = \frac{\theta_m}{N} \tag{2}$$

where N is the gear ratio of the ball screw ($N = \frac{2\pi}{p_b}$, p_b is the pitch of the ball screw).

The dynamics on the ball screw nut can be written as

$$m_n\ddot{x}_1 = f_b - k_n(x_1 - x_2 + x_0) - b_n\dot{x}_1 \tag{3}$$

where m_n is the mass of the nut; k_n is the stiffness of the spring and b_n is the damping of the nut movement; x_2 is the slider displacement ($x_2 = \frac{r(\theta_l+\theta_r)}{2}$, where θ_l and θ_r are the flexion angles of the left and right hip joints and r is the radius of the hip joint); x_0 is the initial displacement difference between x_1 and x_2 when the springs are not compressed.

The force of the cable (f_c) is half of the spring force given by

$$f_c = \frac{k_n(x_1 - x_2 + x_0)}{2}. \tag{4}$$

The total assistive torque on both sides (τ) can be calculated as

$$\tau = 2rf_c. \tag{5}$$

In order to derive the SEA transfer function, we assume that the SEA has a locked-output ($\dot{x}_2 = \ddot{x}_2 = 0$), then we can obtain the following relation by solving (1) to (5):

$$m_1\ddot{\tau} = rN\eta k_n\tau_m - k_n\tau - b\dot{\tau} \tag{6}$$

where $m_1 = m_n + N^2\eta(J_m + J_b)$ and $b = b_n + N^2\eta b_m$ are the equivalent mass and damping of the system, respectively.

Finally, the SEA transfer function is obtained by

$$P(s) = \frac{\tau(s)}{\tau_m(s)} = \frac{rN\eta k_n}{m_1 s^2 + bs + k_n}. \tag{7}$$

In (7), k_n can be calibrated in advance. The other parameters can be identified based on the open-loop response of the D-SEA with blocked output. In Fig. 4(b), we use P_n to represent the identified nominal plant model of the D-SEA, which was obtained with the help of the MATLAB system identification Toolbox in the experiments.

As shown in Fig. 4(b), the motor command (τ_m) of the controller includes the feedforward term (τ_{ff}), the feedback term (τ_{fb}), and the disturbance observation term (DOB, $\widehat{d}$) as

$$\tau_m = \tau_{\text{ff}} + \tau_{\text{fb}} - \widehat{d}. \tag{8}$$

The feedforward term aims to minimize the control effort of the feedback term by scaling the desired force at the approximate D-SEA output [20]. According to the D-SEA transfer function, the feedforward term is designed as follows:

$$\tau_{ff} = r^{-1}N^{-1}\eta^{-1}\tau_d \tag{9}$$

where τ_d is the torque command of the D-SEA.

The feedback term helps to compensate for the unmodeled friction of the SEA [21], which is built as

$$\tau_{fb} = k_p e + k_d\dot{e} \tag{10}$$

where e is the tracking error between the torque command and the actual assistive torque ($e = \tau_d - \tau$); k_p and k_d are proportional and differential parameters tuned in the tests using the MATLAB PID tuner (automatically tuning based on the tradeoffs between overshoot, response time, phase margin, and so on).

The DOB deals with disturbances originating from humans or the external environment. Variations in the plant model are also compensated by the DOB [20]. Disturbances due to the human or external environment (when the output is not locked) are first estimated by multiplying the nominal inverse model of the plant ($P_n{}^{-1}$) and then removed from the motor torque command. The estimated disturbance term is given by

$$\widehat{d} = \tau P_n{}^{-1}Q - \tau_m Q \tag{11}$$

where Q is a low-pass filter that helps attenuate high-frequency disturbances entering the DOB (the cut-off frequency of the liter is represented by f_c). In addition, it is necessary to have a low-pass filter to make the inverse transfer function causal and real-time implementable ($P_n{}^{-1}Q$) to realize the DOB. In this work, we have used a second order Butterworth filter as

$$Q(s) = \frac{1}{\left(\frac{s}{\omega_q}\right)^2 + \sqrt{2}\left(\frac{s}{\omega_q}\right) + 1} \tag{12}$$

where $\omega_q = 2\pi f_c$. In the experiments, f_c was set to 10 Hz.

B. Assistive Strategy

The assistive strategy of the BSE aims to provide the user with the optimal assistance at the best time based on the tasks to be performed. In this work, we proposed an intelligent assistive strategy that can automatically distinguish between walking and lifting tasks so that the user can move freely during walking and receive appropriate assistive torque during lifting. We use the trunk tilt angle (θ_t) and the average flexion angle of the hip

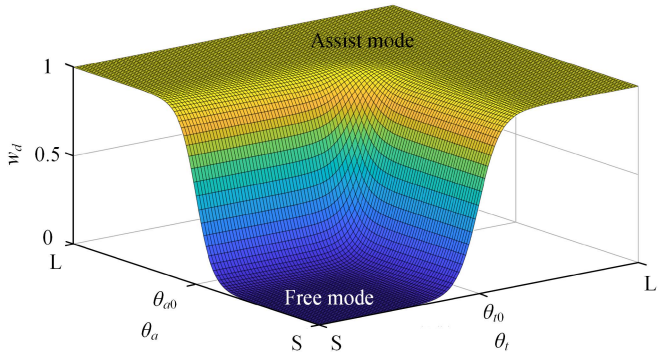

Fig. 5. Switching between the free mode and the assist mode. "S" means small and "L" means large.

joints ($\theta_a = 0.5(\theta_l + \theta_r)$) to distinguish between walking and lifting. The BSE operates in free mode when walking and in assist mode when lifting. By using τ_{df} and τ_{da} to represent the torque command of the two modes, the torque command of the system (τ_d) can be given by

$$\tau_d = (1 - w_d)\tau_{df} + w_d\tau_{da} \tag{13}$$

where w_d is a weight factor related to θ_t and θ_a and is given by

$$w_d = 1 - \frac{1}{(1 + e^{s_d(\theta_t - \theta_{t0})})(1 + e^{s_d(\theta_a - \theta_{a0})})}. \tag{14}$$

In (17), θ_{t0} and θ_{a0} are two angular thresholds and s_d is the sensitivity coefficient of the exponential function. The threshold θ_{t0} can distinguish between walking and stoop-lifting because the human upper body is almost upright when walking [22]. However, θ_{t0} is ineffective in distinguishing between walking and crouch-lifting, because θ_t is small in both walking and crouching. Therefore, we use a different threshold θ_{a0} since θ_a is small in walking but quite large in crouching. In the experiments, θ_{t0} and θ_{a0} were set to 15° and 20° according to the gait data [18]. In real applications, these thresholds can be adjusted according to different working conditions. For example, the angle thresholds can be increased if the worker has to carry goods up the stairs.

The switching between the free mode and the assist mode is shown in Fig. 5. When θ_t and θ_a are both less than the thresholds, w_d is close to zero, then the actual torque command is determined by τ_{df} and the BSE operates in free mode. If either θ_t and θ_a are greater than the threshold, the BSE operates in assist mode. The transition between modes is continuous and smooth, and the speed of the transition is determined by the sensitivity coefficient s_d. In practice, the sensitivity coefficient can be selected based on a tradeoff between the smoothness of the transition (indicated by the overshoot of the force during the transition) and the speed of the transition. An example of calibration of the sensitivity coefficient is repeated division (if the overshoot of the force is acceptable) or multiplication (if the overshoot of the force is very large) of a selected initial value (such as 1) by 0.8 until a suitable value is found.

To achieve active backdrivability in free mode, τ_{df} is set to zero. Then, the torque command of the system can be rewritten as follows:

$$\tau_d = w_d\tau_{da}. \tag{15}$$

In assist mode, we have developed a virtual impedance controller to provide the user with an appropriate assistive torque given by

$$\tau_{da} = K\theta_a - B(\dot{\theta}_a)\dot{\theta}_a \tag{16}$$

where K is the virtual stiffness constant and $B(\dot{\theta}_a)$ is a virtual damping coefficient related to $\dot{\theta}_a$.

The stiffness term represents the static (or quasi-static) torque demand due to the moment of gravity, and the damping term represents the dynamic torque demand due to the user's intention to move. Since the user may requires different damping coefficients when bending and lifting, we designed $B(\dot{\theta}_a)$ as

$$B(\dot{\theta}_a) = (1 - w_b)B_1 + w_bB_2 \tag{17}$$

where B_1 and B_2 are two positive damping constants and w_b is another weight factor, which is given by

$$w_b = \frac{1}{1 + e^{s_b\dot{\theta}_a}} \tag{18}$$

where s_b is the sensitivity coefficient.

In particular, (16) can be rewritten as follows:

$$\tau_{da} = K(\theta_a - B_K(\dot{\theta}_a)\dot{\theta}_a) \tag{19}$$

where $B_K(\dot{\theta}_a) = \frac{B(\dot{\theta}_a)}{K}$ is the new damping coefficient. Then, K can be considered as the assist level of the BSE, which is adjusted according to the user habit and working conditions. In the real application, K and $B_K(\dot{\theta}_a)$ can be set as follow. First, we set $B_K(\theta_a)$ to zero and let the user choose an appropriate assist level during quasi-static lifting. Then, we increase or decrease the damping constants according to the user's feedback during the bending and lifting motions. For example, if a user feels too much force during bending, we increase B_2 to reduce the assistance when $\dot{\theta}_a$ is negative.

TABLE II
VALUE OF THE CONTROL PARAMETERS IN EXPERIMENTS

k_p	0.254	k_d	0.0032	θ_{t0}	15°
θ_{a0}	20°	s_d	2	s_b	1
K	9 Nm/rad	B_1	9 Nm/(rad/s)	B_2	5.4 Nm/(rad/s)
$P_n(s)$	$\frac{42970}{s^2+11.07s+857.3}$				

IV. EXPERIMENT

A. Torque Tracking Performance of D-SEA

A series of experiments were conducted to validate the proposed BSE. All control parameters used in the experiments are listed in Table II. First, the torque tracking performance of the D-SEA was tested, which is important to ensure that the assistance is executed exactly as commanded. The tests of the D-SEA include the following.

1) Effectiveness of the DOB: To test the effectiveness of the DOB, we fixed the left hip joint of the BSE and used a motor-gear mechanism to drive the right hip joint as the disturbance.

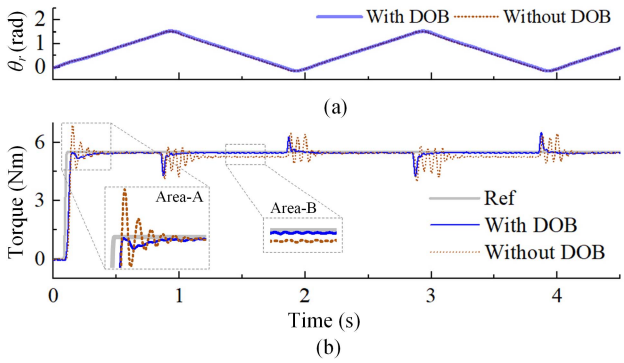

Fig. 6. Effectiveness of the DOB. (a) Actual angle of the right hip joint with and without DOB (driven by a motor-gear mechanism). (b) Torque tracking performance of the D-SEA with and without DOB. The DOB effectively reduced overshoot (Area-A) and steady-state error (Area-B) under disturbance. "Ref" represents the reference torque.

The D-SEA was commanded to track a step torque signal with and without the DOB. The motor-gear mechanism produced the same joint movement with and without the DOB (θ_r from 0 to 1.9 rad) as shown by the actual angle of the right hip joint in Fig. 6(a). The experimental results [see Fig. 6(b)] show that the DOB can reduce the torque tracking overshoot (Area-A) and the steady-state error (Area-B) under the disturbance, verifying the effectiveness of the DOB.

2) Large Torque Tracking Performance: The D-SEA was instructed to track the large torque of a sinusoidal 1 Hz signal. The torque range is from -3 to 30 N $\cdot$ m (spring force from -60 N to 600 N), since the BSE only provides large assistance in one direction. As shown in Fig. 7(a), the experimental results indicate that the D-SEA can accurately track the torque command, with an absolute maximum tracking error of about 0.4 N $\cdot$ m.

3) Zero Torque Tracking Performance: To test the active backdrivability of the D-SEA, we let the D-SEA track the zero torque command under disturbances, which were manually added by the user (by moving the thigh links). The average flexion angle of the hip joints (θ_a) and the tracking errors ($\tau_d - \tau$) are shown in Fig. 7(b). During the fast and long-range movements of the thigh links, the D-SEA showed good backdrivability with a maximum resistance torque of 0.1 N $\cdot$ m. The results confirmed that the D-SEA allows the user to move in free mode with little resistance.

4) Torque Tracking Bandwidth: To validate the torque tracking bandwidth of the D-SEA, we performed the frequency respond test and obtained the Bode plot of the D-SEA, as shown in Fig. 7(c). The Bode plot shows that the torque tracking bandwidth of the D-SEA is up to 11 Hz, which is sufficient for leg movements during lifting and walking. The phase margin is also sufficient within the bandwidth.

B. Assistance in Lifting Works

The assistance of the BSE during lifting operations in a stooping and crouching posture is shown in Fig. 8. The lifting task in the experiment can be divided into three stages (A, B, and C). In stage-A, the subject bent to reach the box (or set the box down if he already had it in his hand) and the assistive torque is close to zero until the stiffness term in (19) is greater than the damping term (the lower limit of the torque command is 0). In stage-B, the subject remained bent over to catch and hold the box, and θ_a is close to zero, so the assistive torque is mainly determined by the stiffness term (the bending angle). The subject lifted the box up in stage-C, and the BSE provided the maximum assistive torque of about 30 N $\cdot$ m in this phase. After standing straight, the subject returned to the natural standing posture to prepare for the next lifting cycle. When lifting in the stooping posture, θ_t is close to θ_a because the subject relied mainly on the movement of the waist to lift the box. When lifting in the crouching posture, θ_t is smaller than θ_a because the subject relied on the leg movement more than the waist movement to lift.

C. Muscle Activities Effect

To validate the effectiveness of the proposed BSE, we conducted a series of tests that simulated industrial lifting tasks and recorded muscle activations using surface electromyography (EMG). The experiments took place at the BioRobotics Lab at the National University of Singapore. Fourteen healthy male subjects (age: 23 $\pm$ 1.2 yo; height: 175.7 $\pm$ 3.5 cm; weight: 75.34 $\pm$ 7.2 kg) voluntarily participated in the experiments. None of the participants reported having a previous low back injury at the time of data collection. The experimental protocol was approved by the Institutional Review Board of the National University of Singapore (NUS-IRB Study LH-20-021). Before the study began, the investigators explained the general purpose of the study and obtained verbal and written informed consent from the participants.

EMG signals were recorded using a Delsys Trigno Wireless System (Delsys Inc., Boston, MA, USA). It differentially amplifies the signals with a gain of 1000 and filters them with a bandwidth of 20–450 Hz. The sampling frequency was set to 2000 Hz. A total of four sites [unilateral on the right side of the erector spinae iliocostalis (ESI) at L2, erector spinae longissimus (ESL) at L1, biceps femoris, and rectus femoris] were observed for EMG measurements. Before performing the tasks, participants performed maximal effort to achieve MVC of the back and leg muscles. The peak values of the linear envelope of the EMG signals were defined as the MVC for each muscle and used to normalize the subjects' EMG data and for comparison between subjects. SENIAM methods were used for the MVC measurements [23]. The tasks included (a) lifting in a stooped position from the floor, (b) lifting in a crouched position from the floor, and (c) walking, as shown in Fig. 9. For the lifting tasks, 10 kg was chosen. The measurement trials were repeated twice, and each trial lasted approximately 20 s. All subjects performed the tasks alternately with and without the exoskeleton. In (a), participants had to lift a box four times from the floor to the upright position with knees extended. In (b), participants had to lift a box from the floor to the upright position four times while bending their knees. In (c), participants walked at walking pace along a 15-m track in similar speed without and with the BSE. During the walking trials, an accelerometer [IMU in Fig. 9(c)] was used to divide the data into cycles to indicate

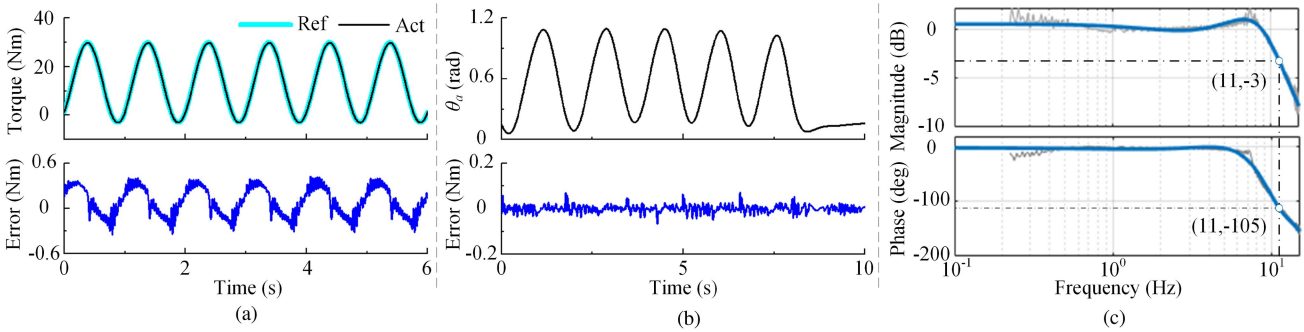

Fig. 7. (a) Large torque (1 Hz, from −3 to 30 N · m) tracking performance of the D-SEA. (b) Zero torque tracking performance of the D-SEA under perturbations (see θ_a, the thigh links were manually moved). (c) Frequency response of the D-SEA. "Ref" represents the reference torque; "Act" represents the actual torque.

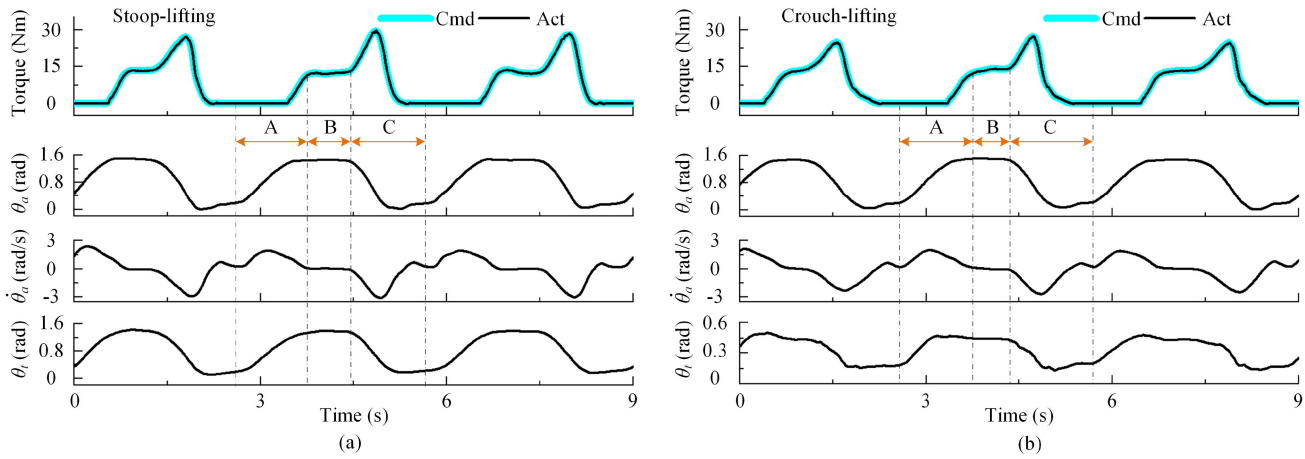

Fig. 8. Assistance of the BSE in lifting works. (a) With stooping posture. (b) With crouching posture. "Cmd" represents the assistive torque command; "Act" represents the actual assistive torque.

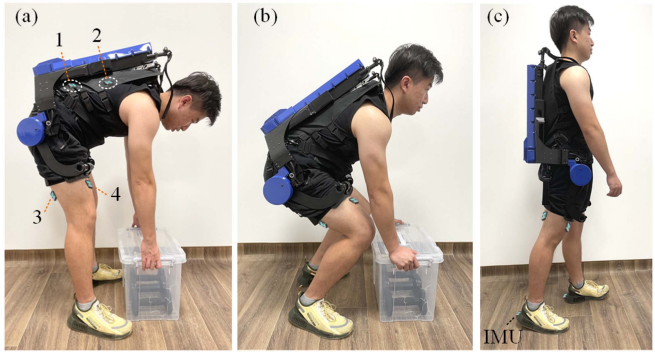

Fig. 9. Muscle activity test in the lifting work and walking. (a) With stooping posture. (b) With crouching posture. (c) Walking. Positions of EMG sensors: 1) ESI; 2) ESL; 3) Rectus Femoris (RF); 4) Biceps Femoris (BF). In the walking test, two IMUs were added to detect heel strike.

heel strike for each epoch of the gait cycle. Wilcoxon signed rank test was used to compare the conditions with and without the exoskeleton, with $p < 0.05$ considered statically significant (using GraphPad Prism software version 9.0, San Diedo, CA, USA).

EMG results (in percent of MVC) of the lifting and walking tests are shown in Fig. 10 and Table III. During lifting in a stooped position, significantly lower mean activations were found in the conditions with BSE compared to the non-BSE conditions of ESI (−7.29% MVC, $p = 0.002$) and ESL (−3.65% MVC, $p = 0.004$). Moreover, the maximal activation of ESI (−24.06% MVC, $p = 0.001$), ESL (−19.67% MVC, $p < 0.001$), and BF (−9.49% MVC, $p = 0.007$) was significantly lower in the condition with BSE. During lifting in a crouched position, significantly lower mean activations of ESI (−8.12% MVC, $p = 0.003$), ESL (−1.4% MVC, $p = 0.003$), and BF (−3.24% MVC, $p = 0.01$) muscles were found in the condition with BSE compared to the condition without BSE. In addition, significantly lower maximal activations of ESI (−25.69% MVC, $p = 0.005$), ESL (−2.69% MVC, $p = 0.004$), and BF (−2.69% MVC, $p = 0.004$) muscles were found with BSE. In walking, significantly lower mean activations of ESI (−1.77% MVC, $p = 0.027$) and ESL (−0.95% MVC, $p = 0.031$) muscles were found, and the maximal activation of ESL (−1% MVC, $p = 0.012$) was significantly lower with BSE. No significant differences in RF and BF activation were observed in walking. In summary, the performance of the BSE in lifting loads is shown in Table II, which is a list of the percent reduction in muscle activity that occurred with the use of the exoskeleton. During lifting, the change in muscle activity associated with the no-exoskeleton condition showed a reduction of up to 30.6% for the mean activations of ESI and ESL and up to 41.74%

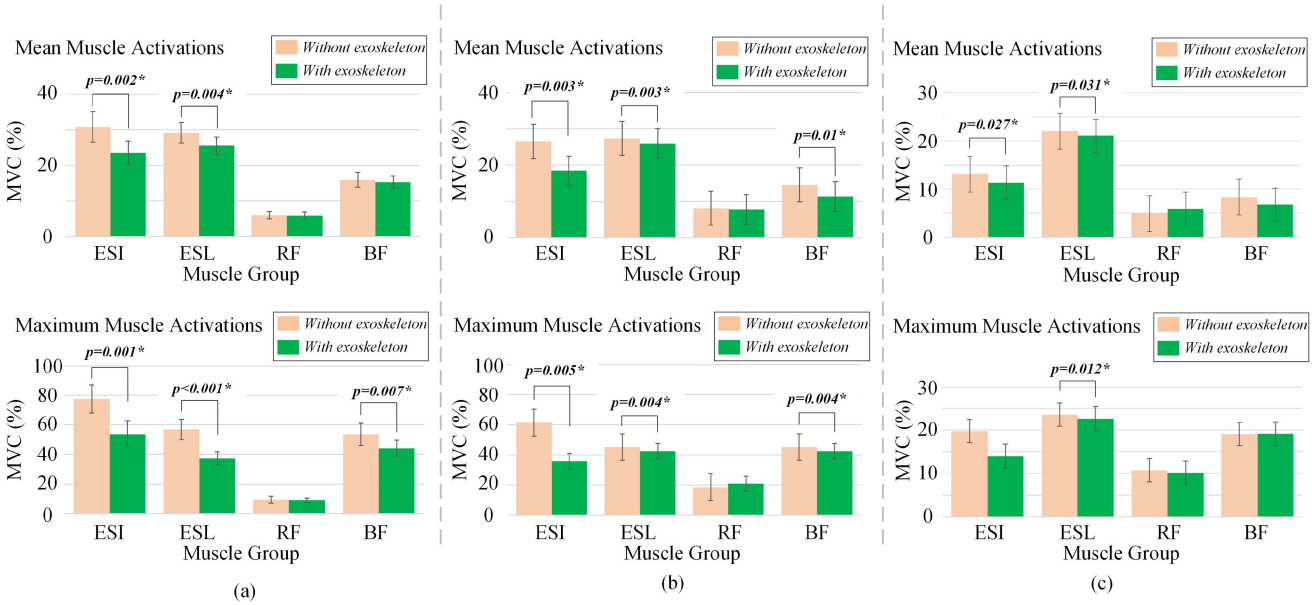

Fig. 10. Statistical results of experimental tasks. ESI: Erector spinae iliocostalis; ESL: Erector spinae longissimus; RF: Rectus femoris; BF: Biceps femoris. The error bars indicate standard deviation intervals, and the symbol * indicates a significant difference between the experimental groups.

TABLE III
REDUCTION PERCENTAGE OF MUSCLE ACTIVITY BY EACH MUSCLE WHEN WEARING THE BSE DURING THE LOAD LIFTING TASK

Muscle Group	ESI	ESL	RF	BF
Lifting with stooping posture				
Mean	23.67%	12.51%	2.69%	4.06%
Max	31.03%	34.55%	4.73%	17.67%
Lifting with crouching posture				
Mean	30.6%	5.13%	5.29%	22.3%
Max	41.74%	5.94%	-11.86%	5.94%
Walking				
Mean	13.48%	4.33%	-21.54%	18.85%
Max	29.05%	4.23%	5.77%	-0.33%

[1] ESI: Erector Spinae Iliocostalis; ESL: Erector Spinae Longissimus; RF: Rectus Femoris; BF: Biceps Femoris

for the maximum activation of them. An interesting result was that the BSE reduced ESI activation by 13.48% in walking. In experiments, we observed that the BSE improved subjects' hunched posture, helping them walk in an upright posture. The improved trunk posture maybe responsible for the reduced ESI activation, since the back muscles is known to restrict excessive trunk movements in walking [10]. No significant changes occurred in leg muscles when walking with the BSE.

V. DISCUSSION

A. Design Innovation

With a D-SEA, we reduce the device weight to the upper limit for a lightweight, portable device (around 5 kg, defined in [24]). In addition to the drive system, the main frame that connects the back and legs is also an important reason for the device weight, as it must be strong enough to transmit the assistive torque. Some SEs directly use the cable to transmit the assistive torque to the user instead of using a frame [12]. However, the force of the cable running parallel to the human back can reach more than 1000 N during the assistance, which is a great stress on the user's lumbar spine. Therefore, many active BSEs still use a hard frame to transfer the assistive torque to the user [25], even though this may increase the weight of the device. We placed the upper connection points of the frame at human shoulder height (adjusted by the sliding link) to reduce the force on the shoulder straps (with a large moment arm) and improve user comfort. In order to achieve high force transmission efficiency, we minimized the number of rollers in the design of the cable-roller mechanism, reducing the force loss caused by the friction. In addition, the mechanism has no cables routed around rollers of different heights, which could increase the risk of the cable falling off the roller [13].

Compared to earlier differential actuator designs typically used in hand exoskeletons (or prosthetic) [26], our D-SEA has the advantage of high-quality force control, which is important for human–robot interaction. For example, the differential actuators with gear mechanisms, whiffle-tree mechanisms and pulley mechanisms only controlled the direction of finger movement (grasp or release) [27], [28], [29]. The differential actuator in [30] added elastic components between the motor and fingers, allowing the gripper to conform to the shape of the object. However, the gripper cannot control the torque at the finger joints. In the experiments, our D-SEA showed accurate torque tracking with 0.4 N · m error (absolute maximum error) when tracking a 1 Hz sinusoidal signal with 30 N · m amplitude. The accuracy of the D-SEA is comparable to that of the SEA on the Valkyrie Humanoid Robot, which showed an absolute maximum error of about 1 N · m when tracking a 0.5 Hz sinusoidal signal with 10 N · m amplitude [21]. The back drive

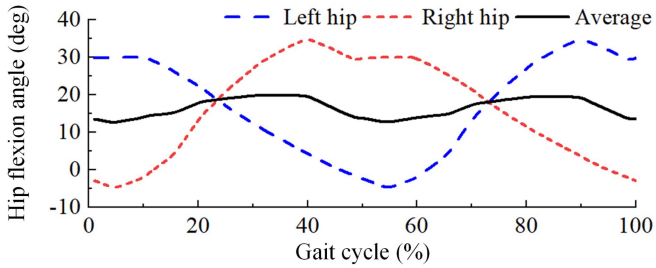

Fig. 11. Left and right hip flexion angles (θ_l and θ_r) and the average (θ_a) during walking according to [18].

torque of the D-SEA is also as low as 3.3 of the output torque. Moreover, the torque tracking bandwidth of the D-SEA (11 Hz) is close to that of other SEAs used for human–robot interaction (5–25 Hz in [31], 16 Hz in [32], and 10 Hz in [33]), and is sufficient to assist lifting motions whose frequency is relatively low. During lifting assistance (see Fig. 8), our assisting torque profile was similar to that of APO [9] and H-WEX-v2 [13], but with different peak values. The optimal assistive torque profile for lifting applications is still a subject of active research. For example, the BSEs in Table I with different assistive torque profiles can all successfully alleviate back muscle fatigue during lifting operations. Therefore, it is important to allow the user to adjust the assistive torque to suit different working conditions and habits (by adjusting K, B_1, and B_2). In (16), we use the angular velocity to detect the lifting and lowering behaviors of the user. Another option available is to use angular acceleration [8], [34] that can achieve better response as it is related to mass and inertia. However, as a derivative of angular velocity, the angular acceleration signal obtained from the sensor may be noisy and easily affected by external forces [35], which affects the control stability. Considering the tradeoff between responsiveness and stability, we selected the angular velocity as the feedback.

A unique feature of our BSE is that the user can walk with low resistance, which is achieved by the good backdrivability of the D-SEA [as shown in Fig. 7(b)] and the intelligent assistive strategy. Other single-motor BSEs have tried to achieve this feature using only the differential mechanism [13], [17], which require the legs to move the same amount in opposite directions during walking ($\theta_l + \theta_r = 0$). However, as shown in Fig. 11, the average of the left and right hip flexion angles varies between 10° and 20°, which is much greater than zero (setting a bias angle cannot solve the problem either due to the changing average). Therefore, the asymmetry of the gait cannot be accommodated using only the differential mechanism. Our BSE can help the user lift the load then carry it to the destination unobstructed, which is of great importance in many workplaces that require cargo handling, such as warehouses, factories, and construction sites.

B. BSE Effectiveness

The results of the preliminary tests showed that the use of the proposed BSE induced a significant reduction in physical strain while performing lifting tasks, as evidenced by reduced EMG activations of back and leg muscles. In the case of back exoskeletons used to assist lifting, the reduction in EMG amplitude of the erector spinae muscle has been widely considered to be the most important unloading effect [5], as this muscle is responsible for straightening the back when bending and standing up, allowing heavy loads to be lifted from the floor. Overall, the BSE appeared to unload the physical demand of the ESI and ESL muscles, ranging from 5.13% to 34.55% and up to 41.74%, independently of the lifting technique. These results correlate well with those of other similar devices (such as [36], [37]). In addition to the positive and expected results in the erector spinae muscles, we found significant EMG reductions in the mean and maximal activations of the biceps femoris during load lifting with flexed knees. The BF is a long muscle in the thigh located in the posterior region that, although not the main motor of the lifting motion, helps in the execution of the crouched lifting motion due to the complicated intermuscular coordination patterns [38]. This could be an explanation for the lower activation of the BF muscles when participants lift the box from the floor to the upright position while bending their knees.

One of the concerns in developing the BSE was the effort required by the user to wear the exoskeleton when performing tasks other than lifting loads (such as walking). When considering the leg muscles (i.e., RF and BF) that play a major role in walking, the BSE was found to provide minimal effort to the user when walking with the device, as evidenced by no change in the activation of these muscles. These results contrast with those of the BNDR exoskeleton [31], which requires users to manually switch between modes, or where muscle activation increased when the user walked with the device. Our results may indicate that unlike many other exoskeletons, our BSE is able to automatically detect lifting from walking, allowing full autonomy to the user and causing minimal additional muscle strain, which is an important innovation in the development of the BSE.

C. Limitations and the Future Work

In our assistive strategy, a weight factor was adopted to classify lifting tasks and walking, which has been proved to be an effective way. The advantage of this strategy is that it uses only few sensors and does not require building a motion database. However, when more motions need to be classified, such as bending over and sitting down, more advanced strategies are required. On the basis of building an offline database of various motions, a support vector machines method [39] can recognize walking, bending, and standing motions. Similarly, the adaptive dynamic movement primitive method [9] may also have good potential to classify different motions of the user. In addition, a machine learning method [40] with multiple sensor inputs have been shown to be effective. Inspired by these methods, our future work will focus on improving the high-level control strategy (adding more sensor inputs and employing machine learning approach) and make the exoskeleton adapt to more motions and work scenarios.

A limitation of our experiments is that most of the participants have no experience with lifting loads. The participation of novices may be considered a limitation of this study, as it is possible that the effects of the exoskeleton may differ from those

of experienced workers. In addition, although the results of back muscle activity validated the effectiveness of the device, more evaluation indicators (such as oxygen consumption, heart rate, and questionnaires) are needed to comprehensively evaluate the device. Therefore, our future work is to evaluate the exoskeleton with skilled workers through various indicators. More aspects of the device, such as the control strategy/parameter, will also be further improved based on worker feedback.

Another interesting topic to discuss is that a user may also need assistance during carrying (walking with the load after lifting it up), since the back muscles are supposed to keep the trunk stable. However, as noted in [10], assisting the back muscles to carry would hinder the leg swing in walking, which is a general limitation of the BSEs. Therefore, more advanced design and control strategies are still needed to assist carrying. In this regard, a BSE with two actuators may have advantages over a BSE with a single actuator, since it can provide independent assistive torques at the hip joints, facilitating the development of complex strategies for assisting carrying.

VI. Conclusion

This article presented the design, control, and validation of an active BSE to assist in lifting loads. The unique design of a differential SEA has made possible a device with small self-weight, balanced assistance (left and right side), and good quality force control. The intelligent assistive strategy automatically distinguishes between lifting and walking, enabling the user to accomplish the work of lifting and transporting. The exoskeleton interaction control test demonstrated that the new BSE is able to provide adequate assistance with a virtual impedance controller. Preliminary tests in the laboratory have shown that the use of the BSE can significantly reduce EMG activations of the major muscles involved in lifting loads. Future work will examine the long-term effects of BSE use in real workers to investigate the effects of systematic use of the BSE on the incidence of MSDs in the back.

References

[1] H. R. Marucci-Wellman et al., "The direct cost burden of 13 years of disabling workplace injuries in the US (1998–2010) Findings from liberty mutual workplace safety index," *J. Saf. Res.*, vol. 55, pp. 53–62, 2015.

[2] J. N. Katz, "Lumbar disc disorders and low-back pain: Socioeconomic factors and consequences," *J. Bone Joint Surg. Amer.*, vol. 88, no. suppl_2, pp. 21–24, 2006.

[3] P. Coenen, I. Kingma, C. R. Boot, J. W. Twisk, P. M. Bongers, and J. H. van Dieën, "Cumulative low back load at work as a risk factor of low back pain: A prospective cohort study," *J. Occup. Rehabil.*, vol. 23, no. 1, pp. 11–18, 2013.

[4] P. Jellema, M. W. van Tulder, M. N. van Poppel, A. L. Nachemson, and L. M. Bouter, "Lumbar supports for prevention and treatment of low back pain: A systematic review within the framework of the cochrane back review group," *Spine*, vol. 26, no. 4, pp. 377–386, 2001.

[5] M. P. De Looze, T. Bosch, F. Krause, K. S. Stadler, and L. W. O'sullivan, "Exoskeletons for industrial application and their potential effects on physical work load," *Ergonomics*, vol. 59, no. 5, pp. 671–681, 2016.

[6] D. J. Hyun, K. Bae, K. Kim, S. Nam, and D.-h. Lee, "A light-weight passive upper arm assistive exoskeleton based on multi-linkage spring-energy dissipation mechanism for overhead tasks," *Robot. Auton. Syst.*, vol. 122, 2019, Art. no. 103309.

[7] J.-H. Park, S. Kim, M. A. Nussbaum, and D. Srinivasan, "Effects of back-support exoskeleton use on gait performance and stability during level walking," *Gait Posture*, vol. 92, pp. 181–190, 2022.

[8] M. Lazzaroni et al., "Evaluation of an acceleration-based assistive strategy to control a back-support exoskeleton for manual material handling," *Wearable Technol.*, vol. 1, pp. e9, 2020.

[9] F. Lanotte, Z. McKinney, L. Grazi, B. Chen, S. Crea, and N. Vitiello, "Adaptive control method for dynamic synchronization of wearable robotic assistance to discrete movements: Validation for use case of lifting tasks," *IEEE Trans. Robot.*, vol. 37, no. 6, pp. 2193–2209, Dec. 2021.

[10] T. Poliero, M. Lazzaroni, S. Toxiri, C. Di Natali, D. G. Caldwell, and J. Ortiz, "Applicability of an active back-support exoskeleton to carrying activities," *Front. Robot. AI*, vol. 7, 2020, Art. no. 579963.

[11] G. Bionics, "Cray x," 2023. [Online]. Available: https://www.germanbionic.com

[12] J. M. Li, D. D. Molinaro, A. S. King, A. Mazumdar, and A. J. Young, "Design and validation of a cable-driven asymmetric back exosuit," *IEEE Trans. Robot.*, vol. 38, no. 3, pp. 1489–1502, Jun. 2022.

[13] D. J. Hyun, H. Lim, S. Park, and S. Nam, "Singular wire-driven series elastic actuation with force control for a waist assistive exoskeleton, H-WEXV2," *IEEE/ASME Trans. Mechatron.*, vol. 25, no. 2, pp. 1026–1035, Apr. 2020.

[14] H. Yu, S. Huang, G. Chen, Y. Pan, and Z. Guo, "Human–robot interaction control of rehabilitation robots with series elastic actuators," *IEEE Trans. Robot.*, vol. 31, no. 5, pp. 1089–1100, Oct. 2015.

[15] F. E. Tosun and V. Patoglu, "Necessary and sufficient conditions for the passivity of impedance rendering with velocity-sourced series elastic actuation," *IEEE Trans. Robot.*, vol. 36, no. 3, pp. 757–772, Jun. 2020.

[16] J.-W. Lee and G. Kim, "Design and control of a lifting assist device for preventing lower back injuries in industrial athletes," *Int. J. Precis. Eng. Manuf.*, vol. 20, no. 10, pp. 1825–1838, 2019.

[17] H. K. Ko, S. W. Lee, D. H. Koo, I. Lee, and D. J. Hyun, "Waist-assistive exoskeleton powered by a singular actuation mechanism for prevention of back-injury," *Robot. Auton. Syst.*, vol. 107, pp. 1–9, 2018.

[18] J. Camargo, A. Ramanathan, W. Flanagan, and A. Young, "A comprehensive, open-source dataset of lower limb biomechanics in multiple conditions of stairs, ramps, and level-ground ambulation and transitions," *J. Biomech.*, vol. 119, 2021, Art. no. 110320.

[19] E. K. Wai, D. M. Roffey, P. Bishop, B. K. Kwon, and S. Dagenais, "Causal assessment of occupational lifting and low back pain: Results of a systematic review," *Spine J.*, vol. 10, no. 6, pp. 554–566, 2010.

[20] N. Paine et al., "Actuator control for the NASA-JSC valkyrie humanoid robot: A decoupled dynamics approach for torque control of series elastic robots," *J. Field Robot.*, vol. 32, no. 3, pp. 378–396, 2015.

[21] N. Paine, S. Oh, and L. Sentis, "Design and control considerations for high-performance series elastic actuators," *IEEE/ASME Trans. Mechatron.*, vol. 19, no. 3, pp. 1080–1091, Jun. 2014.

[22] J. P. Ferreira, M. M. Crisostomo, and A. P. Coimbra, "Human gait acquisition and characterization," *IEEE Trans. Instrum. Meas.*, vol. 58, no. 9, pp. 2979–2988, Sep. 2009.

[23] D. Stegeman and H. Hermens, "Standards for surface electromyography: The European project surface EMG for non-invasive assessment of muscles (SENIAM)," *Enschede: Roessingh Res. Develop.*, vol. 10, pp. 8–12, 2007.

[24] M. Rossini et al., "Design and evaluation of a passive cable-driven occupational shoulder exoskeleton," *IEEE Trans. Med. Robot. Bionics*, vol. 3, no. 4, pp. 1020–1031, Nov. 2021.

[25] S. Toxiri et al., "Back-support exoskeletons for occupational use: An overview of technological advances and trends," *IISE Trans. Occup. Ergonom. Hum. Factors*, vol. 7, no. 3/4, pp. 237–249, 2019.

[26] K. Xu and H. Liu, "Continuum differential mechanisms and their applications in gripper designs," *IEEE Trans. Robot.*, vol. 32, no. 3, pp. 754–762, Jun. 2016.

[27] L. Gerez and M. Liarokapis, "An underactuated, tendon-driven, wearable exo-glove with a four-output differential mechanism," in *Proc. IEEE 41st Annu. Int. Conf. Eng. Med. Biol. Soc.*, 2019, pp. 6224–6228.

[28] A. G. Zisimatos, M. V. Liarokapis, C. I. Mavrogiannis, and K. J. Kyriakopoulos, "Open-source, affordable, modular, light-weight, underactuated robot hands," in *Proc. IEEE/RSJ Int. Conf. Intell. Robots Syst.*, 2014, pp. 3207–3212.

[29] R. R. Ma, L. U. Odhner, and A. M. Dollar, "A modular, open-source 3D printed underactuated hand," in *Proc. IEEE Int. Conf. Robot. Autom.*, 2013, pp. 2737–2743.

[30] M. Shahmohammadi and M. Liarokapis, "A series elastic, compact differential mechanism: On the development of adaptive, lightweight robotic grippers and hands," in *Proc. IEEERSJ Int. Conf. Intell. Robots Syst.*, 2021, pp. 6110–6116.
[31] G. A. Pratt and M. M. Williamson, "Series elastic actuators," in *Proc. IEEE/RSJ Int. Conf. Intell. Robots Syst. Hum. Robot Interact. Cooperative Robots*, 1995, pp. 399–406.
[32] H. Vallery, R. Ekkelenkamp, H. Van Der Kooij, and M. Buss, "Passive and accurate torque control of series elastic actuators," in *Proc. IEEE/RSJ Int. Conf. Intell. Robots Syst.*, 2007, pp. 3534–3538.
[33] K. Kong, J. Bae, and M. Tomizuka, "Control of rotary series elastic actuator for ideal force-mode actuation in human–robot interaction applications," *IEEE/ASME Trans. Mechatron.*, vol. 14, no. 1, pp. 105–118, Feb. 2009.
[34] M. Lazzaroni et al., "Acceleration-based assistive strategy to control a back-support exoskeleton for load handling: Preliminary evaluation," in *Proc. IEEE 16th Int. Conf. Rehabil. Robot.*, 2019, pp. 625–630.
[35] G. Sulligoi and R. Kavanagh, "An innovative method for improved real-time measurements of angular acceleration in motion control systems," in *Proc. IEEE Int. Symp. Power Electronics, Elect. Drives, Autom. Motion*, 2006, pp. 658–662.
[36] M. Abdoli-E, M. J. Agnew, and J. M. Stevenson, "An on-body personal lift augmentation device (PLAD) reduces emg amplitude of erector spinae during lifting tasks," *Clin. Biomech.*, vol. 21, no. 5, pp. 456–465, 2006.
[37] B. L. Ulrey and F. A. Fathallah, "Effect of a personal weight transfer device on muscle activities and joint flexions in the stooped posture," *J. Electromyogr. Kinesiol.*, vol. 23, no. 1, pp. 195–205, 2013.
[38] W. P Lombard and A. D. Kuo, "The action of two-joint," *Classics Movement Sci.*, 2001, Art. no. 289.
[39] T. Poliero, L. Mancini, D. G. Caldwell, and J. Ortiz, "Enhancing back-support exoskeleton versatility based on human activity recognition," in *Proc. Wearable Robot. Assoc. Conf. (WearRAcon)*, 2019, pp. 86–91.
[40] V. Zanina, G. Dlamini, and V. Palyonov, "Deep learning based approach for human intention estimation in lower-back exoskeleton," in *Proc. Adv. Inf. Commun.: Proc. Future Inf. Commun. Conf.*, 2023, pp. 164–182.

Shuo Ding received the B.S. and Ph.D. degrees in mechanical engineering from the School of Mechanical Engineering, Zhejiang University, Hangzhou, China, in 2013 and 2019, respectively.

He is currently a Research Fellow with the School of Biomedical Engineering, National University of Singapore, Singapore. His current research interests include design and control of wearable robotics, human–robot interaction, and sensor network.

Francisco Anaya Reyes received the B.S. degree in biomedical engineering from Tecnológico de Monterrey, Monterrey, Mexico, in 2014 and the Ph.D. degree in biomedical engineering from the National University of Singapore, Singapore, in 2020.

He is currently a Research Fellow with the Biorobotics Laboratory, National University of Singapore. His main research interest are in rehabilitation engineering, functional electrical stimulation, human movement analysis, biomechanics, mobility assistive devices, and global health.

Shounak Bhattacharya received the M.Sc. (Engg.) degree in mechanical engineering from the Indian Institute of Science, Bangalore, India, in 2017.

He is currently a Research Engineer with the National University of Singapore, Singapore. His current work interests include wearable robot, cable driven actuators, structural design.

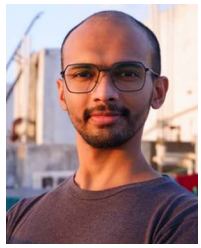

Ashwin Narayan received the B.Tech. degree in electronics and communication engineering from the National Institute of Technology, Tiruchirappalli, India, in 2016, and the Ph.D. degree in biomedical engineering from the National University of Singapore, Singapore, in 2022.

He was a Research Fellow with the Biorobotics Laboratory, National University of Singapore. His research interests include focused on embedded machine learning, intent detection for wearable robots, and real-time embedded systems.

Shuaishuai Han received the Ph.D. degree in control science and engineering with the Nanjing University of Science and Technology, Nanjing, China.

He is currently a Postdoctoral Researcher with the National University of Singapore (NUS), Singapore. His current research interests include the robot-assistive rehabilitation strategies, control of rehabilitation robotics, and series elastic actuator-driven robots.

Seyram Ofori received the B.Sc. degree in biomedical engineering from the University of Ghana, Accra, Ghana, in 2018. He is currently working toward the Ph.D. degree in biomedical engineering with the National University of Singapore, Singapore.

His current research interests include biomechanics testing of wearable industrial robots.

Haoyong Yu (Senior Member, IEEE) received the B.S. and M.S. degrees in mechanical engineering from Shanghai Jiao Tong University, Shanghai, China, in 1988 and 1991, respectively, and the Ph.D. degree in mechanical engineering from the Massachusetts Institute of Technology, Cambridge, MA, USA, in 2002.

He is currently an Associate Professor with the Department of Biomedical Engineering, National University of Singapore, Singapore. His research interests include medical robotics, rehabilitation engineering and assistive technologies, system dynamics and control.